

INVESTIGATION OF DYNAMIC OXYGEN ADSORPTION IN MOLTEN SOLDER JETTING TECHNOLOGY

Constantine M. Megaridis,^{1*} Giulio Bellizia,¹ Michael McNallan¹ and David B. Wallace²

University of Illinois at Chicago,¹ MicroFab Technologies²

Abstract

Surface tension forces play a critical role in fluid dynamic phenomena that are important in materials processing. The surface tension of liquid metals has been shown to be very susceptible to small amounts of adsorbed oxygen. Consequently, the kinetics of oxygen adsorption can influence the capillary breakup of liquid-metal jets targeted for use in electronics assembly applications, where low-melting-point metals (such as tin-containing solders) are utilized as an attachment material for mounting of electronic components to substrates. By interpreting values of surface tension measured at various surface ages, adsorption and diffusion rates of oxygen on the surface of the melt can be estimated.

This research program investigates the adsorption kinetics of oxygen on the surface of an atomizing molten-metal jet. A novel oscillating capillary jet method has been developed for the measurement of dynamic surface tension of liquids, and in particular, metal melts which are susceptible to rapid surface degradation caused by oxygen adsorption. The experimental technique captures the evolution of jet swells and necks *continuously* along the jet propagation axis and is used in conjunction with an existing linear, axisymmetric, constant-property model to determine the variation of the instability growth rate, and, in turn, surface tension of the liquid as a function of surface age measured from the exit orifice. The conditions investigated so far focus on a time window of 2–4ms from the jet orifice. The surface properties of the eutectic 63%Sn-37%Pb solder alloy have been investigated in terms of their variation due to O₂ adsorption from a N₂ atmosphere containing controlled amounts of oxygen (from 8 ppm to 1000 ppm). The method performed well for situations where the oxygen adsorption was low in that time window. The value of surface tension for the 63Sn-37Pb solder in pure nitrogen was found to be 0.49 N/m, in good agreement with previously published work. A characteristic time of O(1ms) or less was determined for the molten-metal surface to be saturated by oxygen at 1000 ppm concentration in N₂.

Introduction

The modern electronics industry is developing a host of emerging technologies, which, when commercialized, are expected to reduce costs and dimensions of electronic devices, while simultaneously allowing a large throughput in electronic assembly. In the past fifteen years, as the integrated chip dimensions decreased, many new challenges have stemmed from the need to assemble these increasingly small components into fully functional entities. Solder Jet Technology or SJT [1] is one such application technique, which relies on inkjet printing principles to create and place monodispersed arrays of molten-solder droplets of approximately 50-100 μm diameter on a substrate containing the electronic circuit. The component is then put in contact with the array of “bumps” of solder deposited on the substrate board and,

Keywords: surface tension, liquid Sn-Pb solder, capillary jet, oxygen adsorption

* Corresponding author. e-mail: cmm@uic.edu

subsequently, the assembly is placed in an oven to remelt the solder and create, after solidification, solid conductive bonds between the parts.

Fluid interface phenomena involving droplet formation from a capillary jet are of central importance in SJT and surface tension is a crucial property affecting jet breakup. Due to the high reactivity of many liquid metals, the presence of surface active elements -even in low concentrations in the local atmosphere- degrades interface tension (σ) [2], which, in turn, compromises the effectiveness of the jetting process. Tin-containing melts are especially susceptible to surface degradation caused by oxygen adsorption [3]. Due to the ubiquitous presence of oxygen in the atmosphere, measurements of surface tension of metal melts exposed to O_2 are needed to assist the commercialization of SJT or other relevant technologies. It is important to note, however, that the time scales in jet capillary breakup are typically near or below a millisecond. This severe requirement disqualifies many standard methods of dynamic surface tension measurement, such as the sessile drop method used by Ricci et al. [4] to determine σ of molten tin over time scales ranging from 0.5 second to hours and in atmospheres with varying oxygen partial pressures. Using capillary jet instability techniques and low melting point metals, one can estimate the surface tension of newly formed surfaces within a time window of a few ms after formation, i.e., when surface properties have not been or are being compromised by adsorbed oxygen. In that sense, jet breakup methods appear to offer an advantage with respect to the temporal resolution afforded in liquid-metal systems, where the kinetics of oxygen adsorption can be quite fast. Although jet instability techniques have been used to determine interfacial tension of aqueous solutions in inkjet printing technology [5], these techniques have not been used to date for low melting point metals.

The experimental method presented herein offers clear advantages in terms of its simple non-iterative nature and its capability to define jet swells and necks at locations distributed *continuously* along the jet propagation axis. The experimental jet shape measurements are used in conjunction with an existing linear, axisymmetric, constant-property model to determine the variation of the instability growth rate, and, in turn, surface tension as a function of surface age measured from the exit orifice. The method is validated using pure water (constant surface tension), and an attempt is made to resolve the surface tension of eutectic 63%Sn-37%Pb solder (melting point of 183°C), as it varies due to O_2 adsorption from a nitrogen atmosphere containing controlled amounts of oxygen. The conditions investigated allow measurements within a time window of 2-4ms from the jet orifice, with temporal resolution down to a fraction of a millisecond. The limitations of the method are discussed, to provide guidance for future investigations in this area.

Theoretical Model

To describe the jet dynamics under the destabilizing action of surface tension, a linear model is adopted with the following assumptions:

- The jet flow is axisymmetric.
- Density ρ and viscosity μ of the liquid are constant over the entire jet length.
- Surface tension varies from one wavelength to the next, but remains constant within the same wavelength.
- The velocity profile is uniform over a cross section.
- Gravity is negligible.
- The drag forces exerted by the surrounding gas on the jet free surface are negligible.
- The disturbance is infinitesimal (i.e., linearity holds).

It is assumed that an infinitesimal radial perturbation, which grows exponentially is applied periodically. Therefore, the radial displacement δ of the jet surface is expected to be of the form

$$\delta(\eta,t) = \delta_0 e^{(\alpha + ik\eta)} \quad (1)$$

where α is the growth rate coefficient, $k=2\pi / \lambda$, and η is the axial coordinate of a reference system moving with the jet velocity.

The previous hypotheses lead to the following dispersion relation [6]

$$\alpha^2 + \frac{2\mu k^2}{\rho I_0(kR_0)} \left[I_1'(kR_0) \frac{2kk^*}{k^2 + k^{*2}} \frac{I_1(kR_0)}{I_1(k^*R_0)} I_1'(k^*R_0) \right] \alpha - \frac{\sigma k}{\rho R_0^2} [1 - (kR_0)^2] \frac{I_1(kR_0)}{I_0(kR_0)} \frac{k^{*2} - k^2}{k^{*2} + k^2} = 0 \quad (2)$$

where the quantity k^* is defined by

$$k^{*2} = k^2 + \alpha\rho/\mu \quad (3)$$

and I_0 , I_1 are hyperbolic Bessel functions of the first kind of order 0 and 1, respectively. The primes in Eq. (2) indicate differentiation with respect to the argument of the function. As predicted by Eq. (2), the interval of instability (where $\alpha > 0$) is $0 \leq kR_0 \leq 1$. Equation (2) was used for the calculation of surface tension when all other parameters were known.

Experimental Apparatus

The apparatus could be operated at any liquid jet temperature between 20°C to 250°C, and included an environmental chamber consisting of an aluminum chamber of dimensions 22×22×25 cm fixed to a stainless steel breadboard.

The upper part of the chamber hosts the jetting device directed downward and mated to the bottom end of the supply reservoir containing the solder. This arrangement minimizes clogging of the device orifice, as most impurities float at the top of the reservoir with mostly clean metal forced through the capillary tube. The jetting device is fabricated by MicroFab Technologies Inc. and its primary component is a borosilicate glass capillary about 3 cm long manufactured by drawing and finely polished at the tapered tip. The orifice diameter is 150μm, which offers the right compromise between two competing requirements: the first, of a small diameter to enhance the effect of surface tension on instability, and the second, of a sufficiently large orifice to avoid capillary clogging by the impurities present in the molten metal alloy.

The jet velocity is controlled by the back pressure applied to the reservoir from the nitrogen tank. The nitrogen environment prevents oxidation at the surface of the liquid metal. From the second tank, a mixture of nitrogen and oxygen is directed into the chamber, while an oxygen analyzer monitors the concentration of the out-flowing gas mixture in real time.

The 63%Sn-37%Pb eutectic solder is heated by the resistors placed all around the reservoir. A real-time feedback control system consisting of the resistors, a thermocouple placed in contact with the solder cartridge and a temperature controller device enables to keep the temperature of the solder within ±1°C of the desired level during the experiment.

The harmonic voltage signal from a function generator is first amplified and then directed to the piezoelectric crystal surrounding the glass capillary, thus exciting the jet in a cyclical manner. The same signal triggers the LEDs placed behind the jet on the back side of the camera. The light source is strobed at the same frequency with the oscillating jet, so that the geometry of the jet surface can be observed clearly in a motionless state. This type of light source has been chosen particularly for the fast response to the voltage applied, yielding a strobe signal of narrow pulse, which is ideal for the current application.

Finally, an oscilloscope monitors the signal driving the piezoelectric crystal and displays the frequency and peak-to-peak voltage. The data from the experiment is produced from the jet images, which are collected using a CCD camera attached to a microscope lens. The typical spatial accuracy of the digitized images is $\pm 3\mu\text{m}$. Another camera, synchronized with the first one, is directed to the oscilloscope screen to record the frequency and voltage associated with each jet image.

Experimental Procedure and Data Analysis

The experimental procedure is a sequence of the following steps. First, the cartridge is filled with solder pellets and closed with a screw-on cap connected to the nitrogen tank. The chamber is closed and the tank valves are opened. Pure nitrogen flows through the cartridge interior, which contains the solder pellets, and reaches the chamber passing through the glass capillary; the controlled mixture of nitrogen and oxygen (if any) from the other tank flows directly to the chamber. When the oxygen concentration in the chamber stabilizes (in about 30 minutes), the heating elements are activated and the temperature of the cartridge gradually rises. When the liquid metal is at the desired temperature, the back pressure in the cartridge is raised and jetting starts. The disturbance introduced by the piezoelectric crystal excites the jet periodically. The velocity and frequency are set to their appropriate values and, finally, images of the jet are captured and stored. Subsequently, the images are processed to compute surface tension at specified spatial stations from the orifice.

Three major factors affect the jet shape, namely, ejection velocity, wavenumber and initial disturbance. The ejection velocity depends on the back pressure applied to the liquid pool. The wavenumber is set by the frequency of excitation of the piezoelectric crystal, while the amplitude of the initial disturbance is set by the applied voltage.

The first restriction imposed for the velocity range is the critical point represented by the partition line between varicose and sinuous breakup regime [7]. For velocities higher than the one corresponding to the critical point, the breakup regime changes from varicose to sinuous, and surface tension is no longer the major factor responsible for instability. In our case, the velocity is kept below that limit and the jet operates always in the varicose instability regime. On the other hand, the spatial growth of the instability is measured and a model for temporal growth rate is applied to determine the value of α . The error of this approach is of the order of β^{-2} [8], where β is defined by

$$\beta = (\rho R_0 / \sigma)^{1/2} U \quad (4)$$

In the above, U denotes the jet exit velocity, while R_0 is the jet exit radius. The β^{-2} accuracy implies that better agreement between spatial instability and temporal instability is expected for high-speed jets. In particular, it is required that $\beta \geq 3$. In the case of 63%Sn-37%Pb solder issuing through a $150\mu\text{m}$ orifice, this translates into velocities greater than about 2.4 m/s; in the reported experiments the velocity was kept in the range $3.5\text{m/s} \leq U \leq 6\text{m/s}$. These velocities, in conjunction with the limited capacity of the solder reservoir, resulted in each solder run lasting less than 2 minutes.

Equation (2) shows that surface tension is inter-related with five parameters, namely, viscosity μ , density ρ , wavelength λ (through the wavenumber kR_0), jet radius R_0 and growth rate α . While viscosity and density are taken from the literature, wavelength, jet radius and growth rate are measured experimentally. The associated errors in σ , due to errors in λ , R_0 and α , have been estimated using a standard sensitivity analysis and the known values for solder $\mu = 0.00195 \text{ Ns/m}^2$ and $\rho = 8218 \text{ kg/m}^3$.

In the present work, the growth rate is calculated by subtracting the radius (or diameter) of necks and swells measured at the *same* axial location. Figure 1 shows how this is achieved. This photo corresponds to an unstable water jet excited at a frequency corresponding to the maximum growth rate (i.e., minimum breakup length). The upper image (a) of the jet is taken without strobing; the image shows two contours. The outer one (separating black from grey) envelops the swells, while the inner one (separating grey from white) envelops the necks. This image shows the lengthwise progression of swells and necks along the jet. The other two images in Fig. 1 (b, c) are composites of (a) and frozen images of the jet outline taken in strobe mode at different phase angles between the function generator (driving the piezoelectric crystal) and the pulse generator (driving the illuminating LEDs). These two image overlays show how necks and swells exactly follow the envelopes identified in the top image. To calculate the growth rate α , we pick several points equally spaced along the axial coordinate (ten, for example), where the corresponding neck and swell diameter difference is calculated. The data obtained in this manner is fitted with an exponential curve ($e^{\alpha z/U}$), from which we determine the value of α applicable to this axial span. Typical axial spans, over which α is measured, extend to about 1.5λ , or in terms to time, to a fraction of a millisecond. These measurements are made at axial locations two to three wavelengths upstream of the drop detachment point, mainly to take advantage of the better definition of the jet outline there compared to locations closer to the orifice.

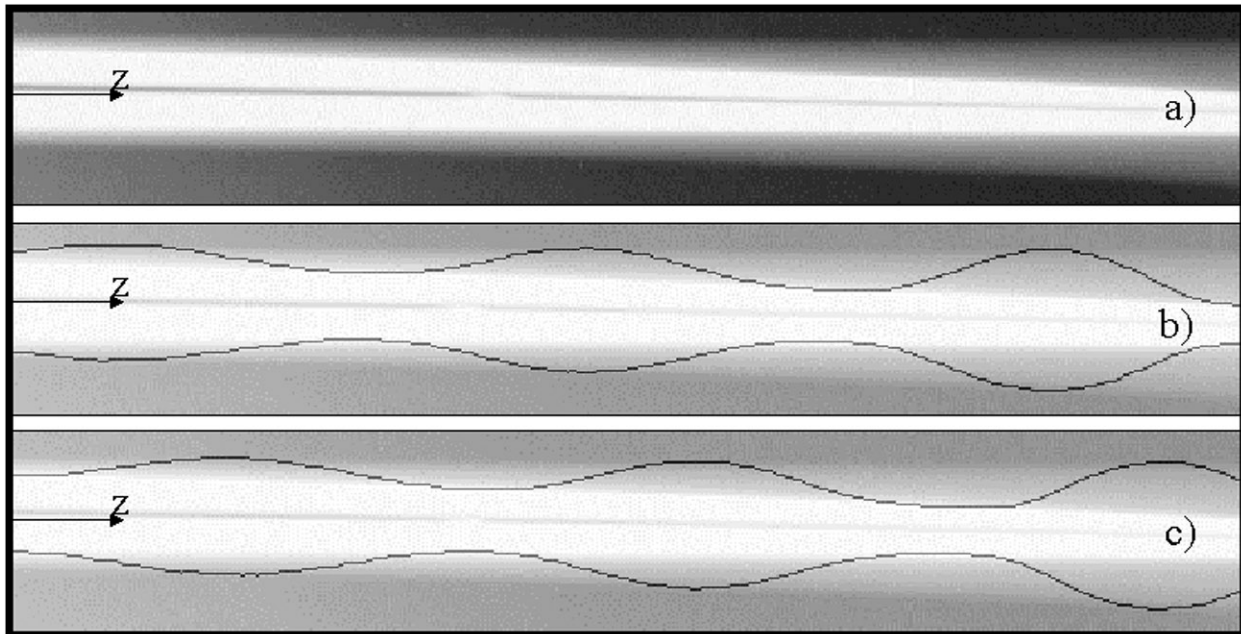


Fig. 1. Experimentally acquired images of an oscillating water jet for the growth rate calculation; a) overlay of many instantaneous images captured by the camera over a time period of 33ms, b) and c) instantaneous (frozen) images overlaid on (a). The slight downward tilt from left to right in all three images is a result of the inclined position of the camera.

The major advantage of this method, in comparison with the method used by Ronay [5], is that the measured value of α is based on a larger number of data stations along the jet length. This translates into a sensible reduction of the statistical scattering. An error analysis [9] showed that given the accuracy of the experimental instrumentation, the error in σ from the experimental uncertainty in determining the jet dimensions was rather high. The alternative way to measure α proposed herein allows not only a reduced error but also the identification of jet segments where the growth rate may no longer be exponential (near the breakup region, for instance).

Method Validation: Experiments with Water

To validate the experimental technique, tests were performed with deionized water, whose physical properties are known; at 20°C $\rho = 998.2\text{kg/m}^3$, $\mu = 1.002 \times 10^{-3}\text{Ns/m}^2$, $\sigma = 7.28 \times 10^{-2}\text{N/m}$. All water experiments were performed at a temperature of 20°C. As stated earlier, each measurement of α (likewise σ) was made over an axial span of $\sim 1.5\lambda$ located two to three wavelengths upstream of the drop detachment point. The average value of σ determined from six water experiments overestimated the actual value of surface tension by 3.8%, which is within the uncertainty, as calculated using standard procedures [9].

Experimental Results for 63Sn-37Pb Solder

The solder used in the experiments is a high-purity eutectic alloy of tin and lead (63%Sn-37%Pb) produced by Witmetaal. This low-melting point material (183°C) is used for electronic components, such as computers and communications equipment, where only moderate heat exposure can be tolerated by the delicate components. The material mass composition analysis, as provided by the manufacturer, is (%): Sn 63.41, Ni ≤ 0.001 , Sb 0.009, Bi 0.006, Cd ≤ 0.001 , Cu 0.001, Ag ≤ 0.001 , Zn ≤ 0.001 , Al ≤ 0.001 , Fe ≤ 0.001 , In 0.002, As ≤ 0.001 , Pb Balance.

Table 1 below lists the conditions for four experiments performed using solder. In all cases, the temperature of the molten metal was maintained at 240°C. For each case, additional information is provided in the table regarding the oxygen content in the nitrogen atmosphere, as well as the surface age at the point of measurement. Surface age is defined as the time period required for the jet to traverse from the orifice to the axial point where each measurement is made. As explained earlier, measurements are made over regions two to three wavelengths upstream of the drop detachment point. It is emphasized that α is measured over an axial span of $\sim 1.5\lambda$, which corresponds to a temporal span of about 0.3ms. So although the measured value of α (likewise σ) corresponds to a time window, the extent of this window (0.3ms) is low enough, such as to consider this measurement instantaneous compared to the longer period ($>2\text{ms}$) required for the fluid to reach the measurement station after exiting the orifice (where surface age = 0). The uncertainty in σ , as listed in the last column of Table 1, was estimated using standard methods [9]. It is apparent that the calculated values of σ for surface ages between 2-4ms are narrowly distributed around 0.49 N/m, which compares favorably with the range of 0.50-0.51 N/m reported in [10] for 60%Sn-40%Pb solder and temperatures between 210-250°C. Carroll and Warwick used a maximum bubble pressure technique to obtain these values. Hoar and Melford [11] used a capillary rise technique to obtain values from 0.535 N/m down to 0.520 N/m in the temperature range of 180 to 230°C for an alloy containing 61.6% Sn by weight. White [12] employed a sessile drop technique and obtained values of 0.480-0.485 N/m for a 60.12% Sn alloy in the temperature range of 220-260°C.

Table 1. 63Sn-37Pb solder data: Experimental parameters and results

O ₂ conc. [ppm]	Surface Age [ms]	Jet Dia. [μm]	Frequency [Hz]	Velocity [m/s]	Growth Rate (α)	Surf. Tension σ [N/m]
20	2.5	147	9135	5.96	4218	0.480±0.027
17	2.0	147	7265	5.13	4186	0.499±0.029
12	2.1	153	8375	4.85	3550	0.480±0.053
8	4.0	153	6000	3.41	3483	0.487±0.075

The surface tension values listed in Table 1 correspond to surface ages in the range 2-4ms. This range was possible by changing the jet exit velocity and using the same solder jetting device, which featured a 150μm-diameter orifice. In principle, surface ages lower than those listed in Table 1 can be attained by either conducting measurements closer to the orifice, or using a smaller diameter orifice. Unfortunately, the latter option was not possible due to the associated increased risk of clogging combined with the limited availability of solder jetting devices in the commercial market. Thus, an attempt was made to conduct measurements closer to the available orifice. It was found that the error in σ increased with distance from the optimum location, which is positioned 2-3 wavelengths upstream from the breakup point. Consequently, this increased error did not allow any definitive conclusions regarding the value of σ at surface ages below 2ms.

It is noted that the oxygen concentration in all four runs of Table 1 is quite low, essentially corresponding to jetting in a nearly pure nitrogen atmosphere. Additional solder experiments have been conducted using an ambient oxygen concentration of 500 ppm (0.05% in nitrogen), with the goal to resolve surface tension variation with surface age. The oxygen surrounding the molten metal jet is adsorbed to the surface, thus lowering the value of surface tension [3]. However, the values of σ obtained under these conditions were low and out of the reasonable range determined from thermodynamic considerations [10]. The unreasonably low values of σ may be due to the excessively simple theoretical model adopted, which is inadequate in those cases in which surface tension changes rapidly along the axial coordinate owing to the adsorption of oxygen from the surroundings. Here, a model that accounts for the coupling effect of both capillary instability and oxygen adsorption, for example, similar to the one proposed by Artemev and Kochetov [13], might give a better description of the dynamics of the disintegrating jet. An additional reason for the poor performance of the present model in cases where O₂ content is non-negligible could be non-uniform oxygen transport rates over swells -as compared to necks- which, in turn, cause variations of σ along a single wavelength. The present model does not consider variation of σ along a single wavelength. Nevertheless, with the present experimental technique, it would be possible to trace the evolution of necks and swells along the axial coordinate and, thus, potentially validate a more encompassing model that accounts for the above chemical or physical transport mechanisms. The identification of such theoretical model is out of the scope of the present effort.

The highest oxygen concentration used in the solder experiments was 1000 ppm (0.1% in nitrogen). Beyond this limit, the surface apparently saturated so quickly that the jet did not respond any longer to the excitation induced by the piezoelectric crystal, irrespectively of the applied frequency and voltage. A concentration of 1000 ppm appears to be the limiting value for controlling the breakup of molten 63Sn-37Pb solder by induced capillary instability under the conditions investigated herein. This result, in turn, suggests a characteristic time of O(1ms) or less required for the molten-metal surface to be saturated by oxygen at this concentration (1000ppm). The kinetic-fluidynamic diagrams for liquid metal-oxygen

systems reported in [14] allow the estimation of the time required to form an adsorbed oxygen monolayer on the melt surface exposed to an inert carrier flow containing definite amounts of oxygen. For molten tin at 232°C, this time was reported to be ~44s at 1ppm O₂ in Helium. If one assumes linearity, the oxygen monolayer formation period at 1000ppm would be 44ms for pure tin, a time period that substantially exceeds the one designated in the present work. This discrepancy may be due to the presence of nitrogen (instead of He) in the current work, or the presence of Pb in the molten multicomponent phase. It may also be attributed to the inherent differences between the two physical configurations, which affect the gas diffusion layer characteristics above the liquid metal surface, and, in turn, the transport of oxygen molecules to it.

Conclusions

An oscillating capillary jet method has been developed for the measurement of dynamic surface tension of liquids, and in particular, metal melts which can rapidly react with surface active elements (such as oxygen) in the ambient atmosphere. The technique captures the evolution of jet swells and necks *continuously* along the jet propagation axis and allows measurement of interfacial tension within a time window of a few milliseconds from the orifice.

The experimental technique was used in conjunction with an existing linear, axisymmetric, constant-property model to determine the variation of the instability growth rate, and, in turn, surface tension of the liquid as a function of surface age measured from the exit orifice. The conditions investigated featured measurements within a time window of 2-4ms from the jet orifice, with temporal resolution down to a fraction of a millisecond. In test experiments conducted with a pure substance (deionized water), the value of σ calculated was well within 5% of the known value. An attempt was made to resolve the surface tension of the eutectic 63%Sn-37%Pb solder alloy (melting point of 183°C), and its variation due to O₂ adsorption from a nitrogen atmosphere containing controlled amounts of oxygen (from 8 ppm to 1000 ppm). The combination of experiment and model performed well for situations where the oxygen adsorption was low in that time window. The values of surface tension for the 63Sn-37Pb solder in a virtually pure nitrogen ambient was found to be 0.49 N/m, a value that is in good agreement with other published studies. However, in cases where oxygen adsorption degraded the melt surface too rapidly, the theoretical model proved inadequate. Despite the shortcomings of the tested model, the experimental technique could be useful in validating a more encompassing model that accounts for the coupling effect of capillary instability and oxygen adsorption (in other words, allows for variation of interfacial tension within a single wavelength).

An oxygen concentration of 1000 ppm was found to be the limiting value for controlling the breakup of molten 63Sn-37Pb solder by induced capillary instability under the conditions investigated herein. This result, suggests a characteristic time of O(1ms) or less required for the molten-metal surface to be saturated by oxygen at this concentration.

Acknowledgement

This work was supported by NASA grant NAG8-1473. We acknowledge the support of MicroFab Technologies in terms of providing equipment and expertise on the jetting instrumentation. Art Sawczuk made contributions to the design of many experimental components, and was responsible for their construction. We also thank Ugur Alakoc for useful discussions.

References

- ¹ Hayes, D. J., Wallace, D. B., Boldman, M. T. and Marusak, R. E., *Int. J. Microcircuits and Electronics Packaging* **16**, 173 (1993).
- ² Keene, B. J., *Int. Mater. Rev.* **33**, 1-37 (1988).
- ³ Passerone, A., Ricci, E. and Sangiorgi, R., *J. Materials Sci.* **25**, 4266 (1990).
- ⁴ Ricci, E., Nanni, L. and Passerone, A., *Phil. Trans. R. Soc. Lond. A* **356**, 857 (1998).
- ⁵ Ronay, M., *J. Colloid and Interface Sci.* **66**, 55 (1978).
- ⁶ Weber, C., *Math. und Mech.* **11**, 136 (1931).
- ⁷ Ohnesorge, W., *Z. Angew. Math. Mech.* **16**, 355 (1936).
- ⁸ Keller, J. B., Rubinow, S.I. and Tu, Y. O., *Physics of Fluids* **16**, 2052 (1973).
- ⁹ Bellizia, G., Measurements of Dynamic Surface Tension of Liquid Solder Using Capillary Instability of Jets, M.S. Thesis, University of Illinois at Chicago, 2001.
- ¹⁰ Carroll, M. A. and Warwick, M. E., *Materials Science and Technology* **3**, 1040 (1987).
- ¹¹ Hoar, T. P. and Melford, D. A., *Transactions of the Faraday Society* **53**, 315 (1957).
- ¹² White, D. W. G., *Metallurgical Transactions* **2**, 3067 (1971).
- ¹³ Artemev, B. V and Kochetov, S. G., *J. Eng. Phys.* **60**, 425 (1991).
- ¹⁴ Ricci, E., Passerone, A., Castello, P. and Costa, P., *J. Materials Sci.* **29**, 1833 (1994).